steel research international

Combinatorial Alloy Design by Laser Additive Manufacturing

Helene Knoll, Sörn Ocylok, Andreas Weisheit, Hauke Springer, Eric Jägle, and Dierk Raabe*

The authors uses laser additive manufacturing (LAM) as a combinatorial method for synthesizing microstructurally and compositionally piecewise graded bulk alloys. Authors fabricate blocks consisting of a sequence of ≈500 μm thick tool steel layers, each with different chemical composition, by laser metal deposition where alloy powders are deposited layer-wise on a substrate. The reference materials are a Cr–Mo–V hot working tool steel and a Ni-based maraging steel. The layers between them consist of corresponding blends of the two materials with varying composition from layer to layer (alloy volume fractions 80:20, 60:40, 40:60, and 20:80). The bulk alloy is hot rolled and heat treated. Subsequently each layer is characterized for microstructure, chemical composition and mechanical properties using electron back scatter diffraction, tensile testing, and indentation. The approach is an efficient high-throughput method enabling rapid probing of novel compositional alloy blends. It can be applied for finding new alloys both, by LAM and for LAM. For the tool steel blends synthesized here, authors observe that the Cr–Mo–V tool steel, when mixed with the Ni-base maraging steel, can be continuously tuned for a strength-ductility profile in the range of 800–1650 MPa strength and 15–25% tensile elongation.

1. Introduction and Motivation

1.1. Goal of the Study

We present a new methodology for rapid bulk alloy screening combining two metallurgical research fields, namely, Laser Additive Manufacturing (LAM)[1–13] and combinatorial bulk alloy design.[14–23] As an example system we investigate different alloy blends of two types of tool steels, a Cr–Mo–V hot working tool steel and a Ni-based maraging steel.[24–27] Several earlier papers have also explored different kinds of pathways for synthesizing gradient alloy combinations by using LAM methods. Although some of these earlier methods did not impose additional thermal mechanical processing after the deposition of alloys with compositional gradients, these studies revealed the capability of using additive manufacturing to explore combinatorial bulk samples.[28–31]

Here, we pursue three targets: The first one is to learn how efficiently these two methods can be merged for rapid alloy screening. The second one is to identify tool steel compositions with improved mechanical properties relative to the reference materials. The third one is to screen suited gradient strategies for applications, which require different microstructures and properties in different layers of the same engineering component. The latter goal is important particularly in the field of tool steels, where often very hard surface layers must be combined with more compliant bulk material beneath. LAM is a technique, which is suited to systematically study all these aspects, enabled through its capability of producing complex parts directly from digital blueprints using two groups of alloy powders.

1.2. Combinatorial Metallurgical Thin Film and Bulk Alloy Design Methods

High-throughput methods amenable to combinatorial alloy design were typically based on thin film synthesis, for efficiently probing compositional ranges, for example, for identifying novel intermetallics, shape memory alloys, corrosion protection layers or shape change materials.[32–38] Thin film high-throughput and the associated compositional combinatorial approaches have been developed particularly for the design of functional materials, where

[*] D. Raabe, H. Knoll, H. Springer, E. Jägle
Department for Microstructure Physics and Alloy Design, Max-Planck-Institut für Eisenforschung, Max-Planck-Str. 1, 40237 Düsseldorf, Germany
Email: d.raabe@mpie.de
S. Ocylok, A. Weisheit
Fraunhofer Institut für Lasertechnik (FhG – ILT), Steinbachstraße 15, 52074 Aachen, Germany

DOI: 10.1002/srin.201600416

the intrinsic composition-dependent material behavior, such as conductivity or transformation temperature is more important than properties that depend strongly on microstructure such as strength.

In contrast to these approaches, developing materials for structural applications requires tuning both, intrinsic material parameters, such as stacking fault energy[17–23] or elastic constants[39–41] on the one hand and on the other hand material parameters on microstructural length scales that determine the mechanical response, such as interface density, particle dispersion, dislocation and cell substructure, crystallographic texture, and dual phase properties.

While intrinsic material parameters depend essentially on the bulk chemical composition, microstructure and its evolution upon processing depend on both, composition and the entire thermomechanical history and microstructure inheritance.

Those specific length scales of the microstructure that matter for tuning strength, toughness, and ductility of metallic alloys reach from nanometers (e.g., interface decoration and particle dispersion[42–46]) up to the micrometer regime (e.g., grain size and local texture). These exemplary microstructure-property relations show that the characteristic length scales that are relevant for the mechanical response of alloys are typically larger than the dimensions that can be probed by thin film combinatorial methods.

Conventional bulk metallurgical approaches for probing multiple new variants of structural alloys are, however, rather time consuming as they require screening of a substantial range of variables including bulk synthesis of samples with different composition, deformation, homogenization heat treatment, quenching, recrystallization, precipitation, phase transformation, elemental partitioning, and/or aging.[17] This bulk combinatorial metallurgical screening method, referred to as Rapid Alloy Prototyping (RAP), has been recently introduced and successfully applied to density reduced TWIP-type steels,[17,18] high entropy alloys,[19,20] high strength and martensitic steels,[21,22] and high modulus steels.[47,48] It is a semi-continuous high-throughput bulk casting, rolling, heat treatment, and sample preparation technique, which allows synthesizing and testing up to 45 material conditions within 35 h.

Here, we study an alternative and efficient high-throughput screening method suited for bulk metallurgical alloy design offered by LAM.

1.3. Laser Additive Manufacturing for Combinatorial Metallurgical Alloy Design

For the field of combinatorial metallurgical alloy design, LAM offers a number of advantages over other bulk RAP methods.

First, it imposes a specific thermal pathway during metallurgical synthesis:[1,13] The time-temperature profile experienced by a sample produced by LAM is very different from the one produced by conventional metallurgical manufacturing.[49–53] When a thin powder layer is melted and deposited, the material is quenched at high rates due to rapid heat conduction into the underlying material. Upon deposition of subsequent layers, the consolidated material is repeatedly re-heated and even partially re-melted by the laser beam.[1–4] This means that materials that are synthesized by LAM, undergo sequential series of short pulsed temperature cycles, decaying in intensity with every subsequent deposition layer.[54–63] Such intrinsic heat treatments can be used, for example, for solid-state transformations after deposition. This is of particular interest in the field of tool steels and related alloys, where strength, toughness, and hardness are tuned by precipitating finely dispersed particles.[24–27]

A second advantage of using LAM for combinatorial alloy design is that it involves rapid melting and solidification with only a small melt pool volume.[1–13] This offers the opportunity to also probe materials that cannot readily be cast conventionally, for example, oxide-dispersion strengthened alloys or materials containing solute contents above the solubility limit. Typical cooling rates encountered in LAM range from 10^3 to 10^6 K s^{-1}.[3–13] Such high cooling rates lead to rapid solidification of the melt, yielding beneficial, very fine solidification microstructures, in contrast to the usually coarse casting microstructures obtained after the first step of conventional processing.[55–63] This fact implies that LAM is not only suited as a general tool for combinatorial alloy screening, but also particularly appropriate for probing alloy variants for the field of additive manufacturing.

Third, some LAM methods allow RAP, i.e., quickly screening through a series of compositions. This is due to the powder metallurgical origin of the manufacturing process.[1–4] By introducing a mixture of two or more powders into a pre-mixing chamber, and then into the melt pool, homogeneous alloys of varying composition can be synthesized. In contrast to conventional liquid metallurgical processing, where casting bulk samples with systematically varying alloy composition is very time consuming, LAM enables to produce parts of different composition in one single production step. Also production of graded parts, i.e., with a composition varying within the part, is possible for some of the LAM methods. This RAP ability can be used in the development of materials employed in conventional manufacturing as well as in the development of materials suitable for LAM itself.

1.4. Laser Metal Deposition for Combinatorial Alloy Design

Laser-based Additive Manufacturing of metallic components can be achieved either by Selective Laser Melting (SLM) or by Laser Metal Deposition (LMD).[1–13] The latter approach is sometimes also referred to as Laser Surface Cladding or Laser Cladding.

In SLM, a laser beam is scanned over a powder layer, melting it locally. After the shape of the part has been deposited in that layer and the molten material has solidified, a new powder layer is spread and the process is repeated. Via SLM, parts with almost no restrictions in complexity can be produced. However, SLM needs a monolithic powder (either an alloy or a pre-mixed powder blend), therefore, chemical gradients within a part cannot be produced. Furthermore, the size of the part is limited by the size of the process chamber, i.e., in state-of-the-art instruments to dimensions of about $700 \times 400 \times 500\,mm^3$.

In the LMD process, the metallic powder to be melted and consolidated is introduced into the interaction zone of the laser beam and the substrate through injecting it through nozzles into the melt pool generated by the laser beam, **Figure 1**.[3,6,8,64,65] As carrier gas for the powder an inert gas (e.g., Ar) is used.

The shape complexity accessible with LMD is limited due to the fact that the part is not built up in a supporting powder bed, such as in SLM and also due to the larger laser focus diameters and, hence, melt pool sizes compared to SLM. However, LMD enables building up of continuously or piecewise compositionally graded materials and allows in-situ production of new alloys, which are not necessarily made from pre-alloyed metallic powders, rendering it an ideal tool for efficient and rapid alloy development. Additional advantages of LMD over SLM in the context of combinatorial metallurgical synthesis are the much higher deposition rates of material (typically 10–40 $cm^3\,h^{-1}$ versus 2–10 $cm^3\,h^{-1}$ for SLM) and the size of the part that is not limited by a process chamber.[3,6,8,64,65] Hence, larger shapes can be produced such as, for example, turbine blades with a length of 1 m and more. In the context of structural alloy development, this feature offers a specific advantage, since the method enables manufacturing samples large enough for subjecting them to downstream thermomechanical processing operations. Owing to these features, we introduce in this study LAM as an accelerated and efficient technique for rapidly exploring complex metallurgical bulk alloy spaces.

Up to now, LMD had found its application mainly in the fields of wear protection, repair, and maintenance of high value parts, such as tools, molds, and aerospace components made from Fe-, Ti-, and Ni-based alloys.[3,6,8,64,65] During the 1990s, LMD attracted interest as a manufacturing technique for the first time. Published investigations on LMD as an AM technology are limited to established structural materials, such as low alloyed steel (e.g., 1.2343), stainless steel (e.g., 1.4571), titanium alloys (e.g., TiAl6V4), or cast aluminum alloys (e.g., AlSi10Mg).

2. Materials, Synthesis, Processing and Characterization

2.1. Combinatorial Alloy Screening for the Case of Tool Steels

We have chosen two types of tool steels as starting points and reference materials for synthesizing corresponding alloy blends by LMD, cf. **Table 1**.

One of the reference alloys is a Cr–Mo–V high performance hot working tool steel (tradename Dievar owned by Böhler-Uddeholm Deutschland GmbH, Düsseldorf, Germany), which is characterized by good resistance to heat, cracking, hot wear, and abrasion during tool operation. The second reference alloys is a maraging steel, which

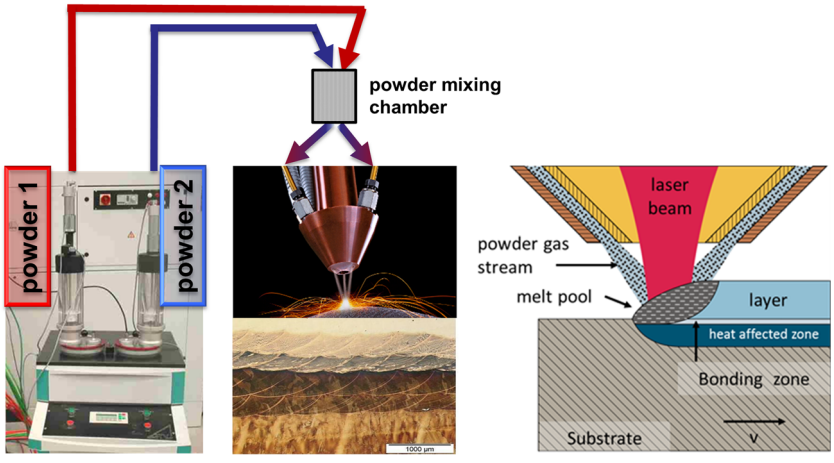

Figure 1. In the Laser Metal Deposition (LMD) process the pre-mixed metallic powder to be melted and consolidated is introduced into the interaction zone of the laser beam and the substrate through injecting it through nozzles into a carrier plasma gas. Corresponding alloy blends among the two powder compositions can be achieved by fractionized contribution from the two different feeding powders of different alloy compositions. Powder mixing is achieved in a separate chamber prior to injection. The figure was reproduced with permission from refs.[6,64]

Material	Content of alloying elements [wt%]									
	C	Cr	Fe	Ni	Co	Mn	Mo	V	Si	Ti
Maraging steel 1.2709 Marlok 1650 °C (Reference alloy 1)	0.008	0.20	Base	14.00	8.00	0.10	5.00	–	0.10	1.00
Tool steel Dievar (Reference alloy 2)	0.35	5.00	Base	_	_	0.50	2.30	0.60	0.20	_
Tool steel alloy 1.2343 (Substrate material)	0.39	5.15	Base	_	_	0.40	1.25	0.38	1.05	_

The tradename Dievar is owned by Böhler-Uddeholm Deutschland GmbH, Düsseldorf, Germany and the tradename MARLOK by Tevo Lokomo Oy, Tampere, Finland.

Table 1. Chemical compositions of two types of tool steels, which were selected as reference materials for synthesizing corresponding alloy blends by LMD and of the substrate steel.

combines very high yield strength and toughness through a near-cubic martensitic matrix microstructure containing a high number density of nm-sized intermetallic precipitates. These nanoparticles are formed after quenching during subsequent ageing at temperatures below the martensite-to-austenite reversion temperature. Here, we use a standard Fe–Ni–Co 1.2709 maraging steel (tradename MARLOK owned by Tevo Lokomo Oy, Tampere, Finland). In this material, hardening takes place after ageing, which makes this material amendable to LAM synthesis owing to the repeated heat exposure during sequential layer synthesis. The synthesis of maraging steels via LAM is well established.[59,66–68] It was observed that the as-deposited material is often in solid solution state. Kempen et al.[67] investigated the SLM manufacturing of 1.2709 maraging steel (Fe–18Ni–5Mo–0.7Ti). It was observed that dense parts could be synthesized when using adequate processing parameters. In accordance with the observations reported by Cabeza et al.,[66] they revealed that the maximum mechanical strength of the steel could be obtained by subsequent age hardening. However, the hardness of the material in the as-produced state was found to be significantly higher than that of conventionally-produced material.

These specific features of the two alloys and the experience with synthesizing them by LAM motivated us to use them as reference materials for conducting an LAM-based high throughput probing of corresponding tool steel alloy blends.

2.2. Laser Metal Deposition and Thermomechanical Treatment

Figure 1 shows the synthesis principle of the LMD approach used in the present study.[6,64] The laser beam melts a thin layer of the substrate, as well as the introduced powder particles, thereby, depositing a layer with nearly 100% density and metallurgical bonding to the substrate.[8] The powder is fed by a disc feeder in a carrier gas stream of argon or helium. This kind of feeder limits the minimum particle size of the powder to 20 μm as smaller particles exhibit an insufficient flow ability due to agglomeration. The carrier gas also shields the melt pool from the surrounding atmosphere. By sequentially depositing layer upon layer, the 3D bulk part is gradually synthesized.

The change in chemical composition of the bulk sample is achieved by feeding the two reference tool steel powders simultaneously into the melt pool, yet, with varying composition through applying varying powder feed rates among the mesoscopic layers to achieve steels with different composition, Figure 1. The resulting samples then exhibit a homogeneous microstructure on a microscopic level inside each compositionally homogeneous layer, but a graded microstructure on a macroscopic level.

Material	Configuration [wt%]	
	Maraging steel 1.2709 Marlok 1650 °C (Reference alloy 1)	Tool steel Dievar (Reference alloy 2)
Alloy 1	100	0
Alloy 2	80	20
Alloy 3	60	40
Alloy 4	40	60
Alloy 5	20	80
Alloy 6	0	100

The tradename Dievar is owned by Böhler-Uddeholm Deutschland GmbH, Düsseldorf, Germany and the tradename MARLOK by Tevo Lokomo Oy, Tampere, Finland.

Table 2. Compositional fractions among the two types of tool steels, which were selected as reference materials for synthesizing corresponding alloy blends by LMD.

In the present approach, by sequentially varying the relative fractions of the two tool steel alloys, six different alloy compositions were deposited layer-wise in one bulk sample by using a 5-axis LMD handling system equipped with a 2 kW fiber-coupled diode laser LDF 1000–2000 in conjunction with a focus diameter of 1 mm.[6,64] During sample production, the powder was fed into the interaction zone flooded with helium to create a protective environment and avoid oxidation of the powders and surface regions.

Block-like specimens with dimensions $30 \times 20 \times 5$ mm^3 have been built up on a substrate consisting of steel 1.2343. The alloys were comprised of a mixture of two components, whose chemical composition is given in Table 1. Synthesis was carried out by feeding variations of the reference constituent powders, cf. **Table 2**.

After LMD synthesis, the multilayer sample was subjected to a total warm deformation of 50% thickness reduction at 1100 °C in a deformation dilatometer DIL 805 A/D (TA Instruments, formerly Bähr-Thermoanalyse GmbH, Germany) equipped with the software WinTA 7.0. Deformation was conducted normal to the TD-LD plane (TD: transverse direction; LD: longitudinal direction) of the compound, i.e., along the build direction (BD) in two passes. The sample was heated in vacuum at a rate of 2 °C s^{-1} to 1100 °C, held at that temperature for 60 s, and subsequently compressed at a strain rate of 0.9 s^{-1}. After a holding time of 120 s, the second deformation step was carried out at a strain rate of 1.1 s^{-1} and followed by a

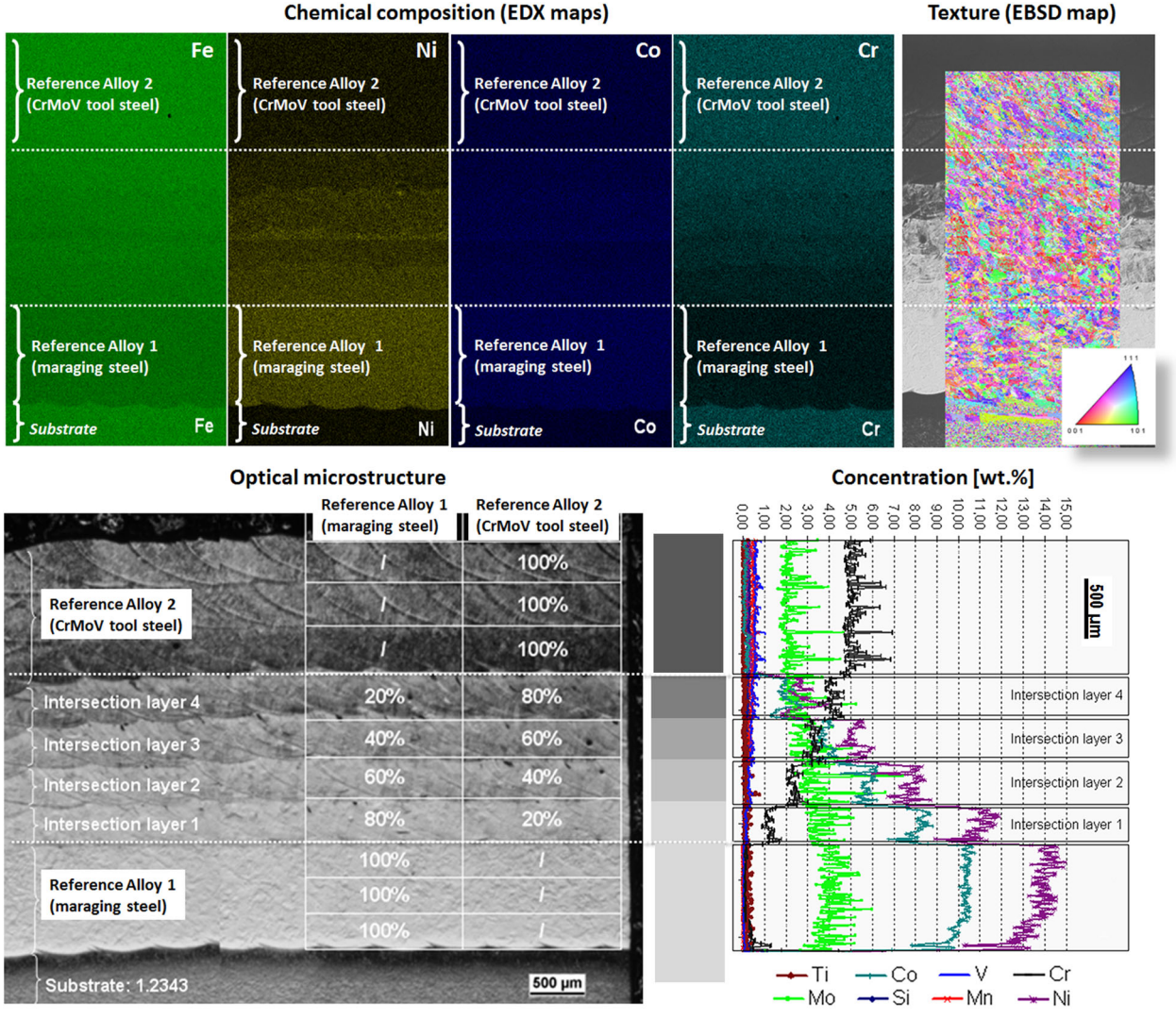

Figure 2. Composition and microstructure overview of the different layers in the bulk graded multi-layer Laser Metal Deposition specimen after subsequent 50% hot thickness reduction conducted at 1100 °C. The respective volume fractions of the tool steel blends can be discerned from the compositional transitions revealed by the color-coded EDX maps. The EBSD cross sectional overview map shows no substantial texture differences among the alloys.

holding time of 300 s. The sample was then manually cooled under argon atmosphere.

2.3. Microstructure and Property Characterization

Analysis of cross-sectional portions of the blended alloys was conducted in the plane perpendicular to the compression direction by grinding and polishing with standard metallographic techniques. Microstructure characterization was carried out by scanning electron microscopy (SEM Zeiss 1540XB). Phase and crystallographic texture mapping was performed on polished samples via electron backscatter diffraction analysis (EBSD; OIM software v.7; 0.05 μm step size) in an SEM Jeol JSM 6500F.

Energy dispersive x-ray analysis (EDX) was conducted for revealing the chemical compositions of the different layers.

For tensile testing, bone-shaped samples were taken from all alloys. The samples were cut parallel to the transversal LD-BD plane by means of electrical discharge machining (LD: longitudinal direction; BD: build direction (normal direction) parallel to the compression direction), such that each tensile testing specimens is taken from one deposited and deformed layer and, thus, corresponds to one particular chemical composition. Before tensile testing, specimen surfaces were coated by a white paint to avoid surface reflections. The white coatings were then decorated with a stochastic graphite aerosol pattern for conducting digital image correlation (DIC) using the ARAMIS system by GOM (GOM: Gesellschaft für Optische Messtechnik mbH, 38106 Braunschweig, Germany).[69–72]

Tensile tests were performed at ambient temperature by means of a deformation device system DDS (Kammrath & Weiss GmbH, 44141 Dortmund, Germany), equipped with a tensile stage. The maximum capacity of the used load cell was 5000 N. The cross head speed was 5.0 μm s^{-1} translating to an initial strain rate of 10^{-3} s^{-1}. The deformation of the samples during elastic-plastic loading was quantified using DIC.[73–75]

Images of the sample surface were captured at time intervals of 2 s using two digital CMOS cameras (DALSA, Waterloo, Canada), which were fixed

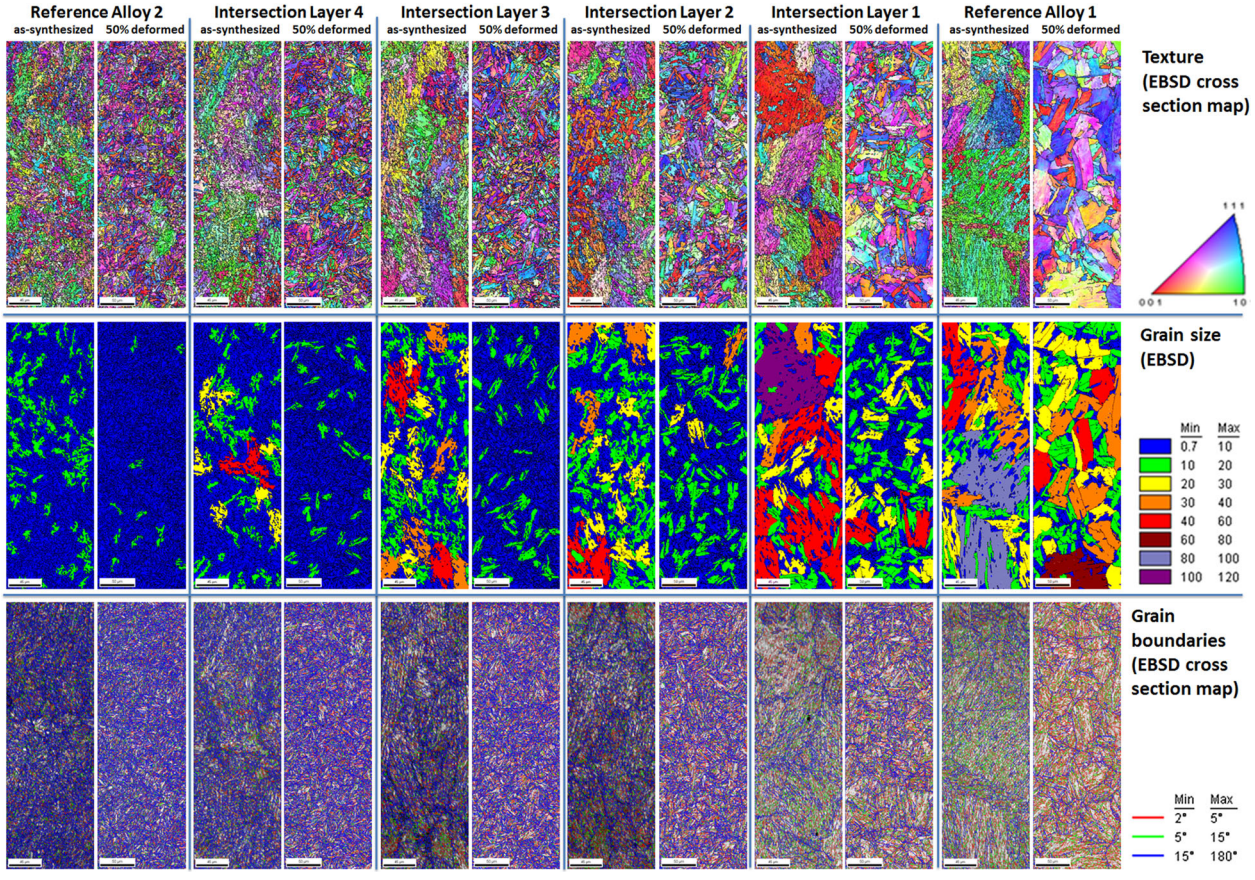

Figure 3. Microstructure and crystallographic texture in terms of detailed EBSD maps taken on all individual alloy layers both, before and after 50% hot rolling at 1100 °C. Some microstructure differences among the different layers become visible which are attributed to the differences in composition and hence martensite start temperature. Top row: EBSD maps; middle row: Grain size maps using high angle grain boundaries; Bottom row: Grain boundaries of different misorientation angle.

perpendicular to the tensile stage. The cameras had a maximum resolution of 2352×1728 pixels and were equipped with lenses of 100 mm focal length maximum aperture of 2.8 (Schneider-Kreuznach, 55543 Bad Kreuznach, Germany). The images were analyzed by means of the ARAMIS software version 6.3.0-5 (GOM, Gesellschaft für Optische Messtechnik GmbH, 38106 Braunschweig, Germany).

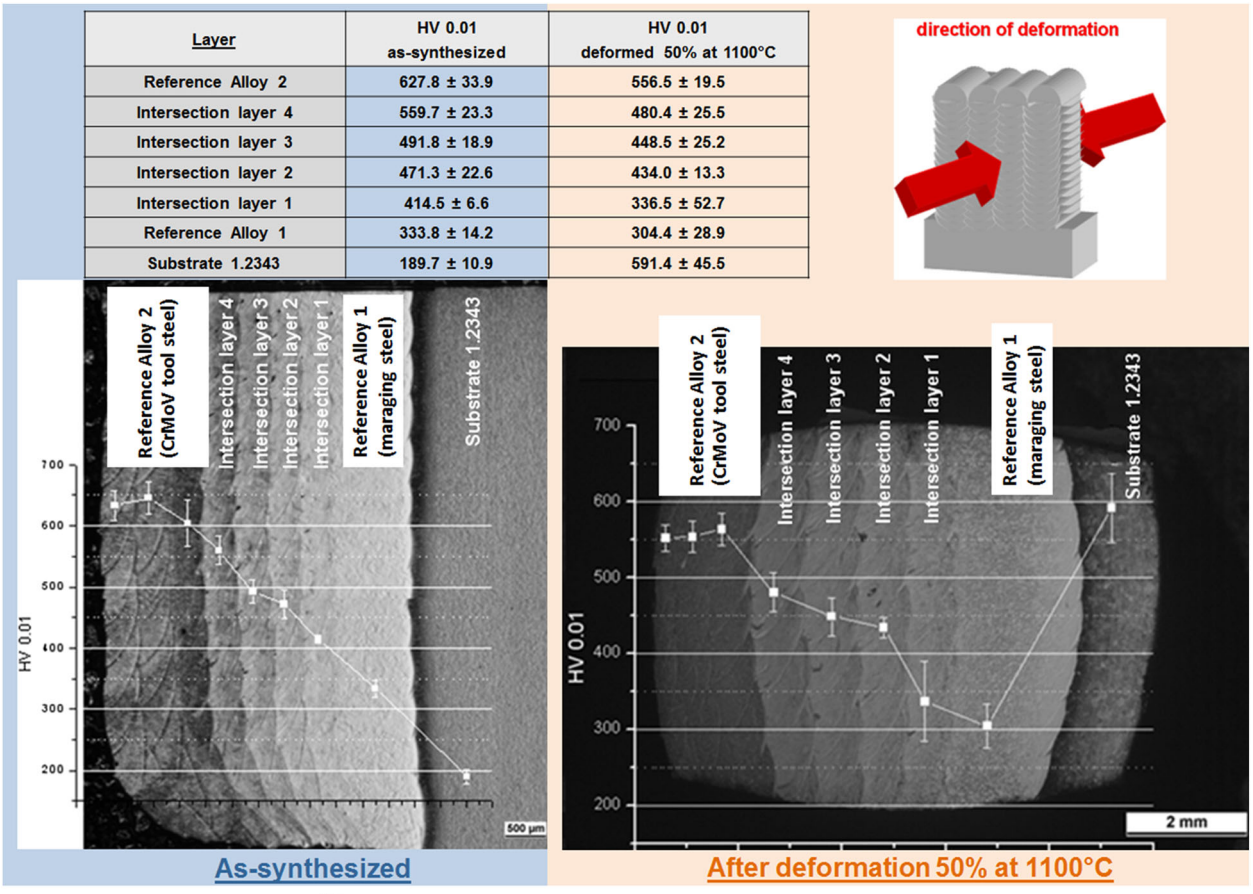

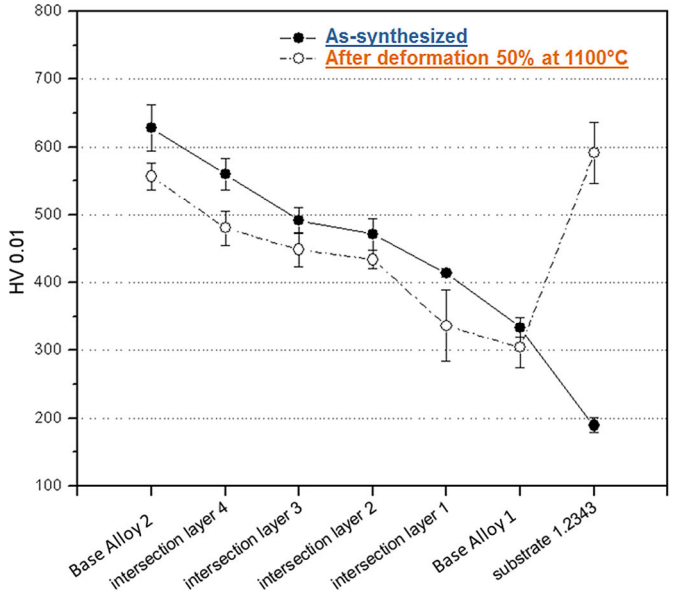

Figure 4. Results from microhardness tests, which were performed both in the as-synthesized state and also after the thermomechanical deformation (50% thickness reduction at 1100 °C) conducted in a dilatometer. The hardness results show a gradual decrease from the CrMoV reference tool steel toward the maraging reference material and the substrate.

3. Results and Discussion

Figure 2 provides a composition and microstructure overview of the different layers in the bulk graded multilayer specimen. Only few pores are observed at this optical resolution, which is attributed to the dense primary synthesis and also to the subsequent 50% hot thickness reduction. The respective volume fractions of the tool steel blends can be discerned from the sharp compositional transitions among the layers and from the contrast change revealed in the optical overview micrograph (etchant: Nital) in Figure 2. The chemical compositions for the different layers are also clearly revealed by the color-coded EDX maps. The distinct compositional transitions between the different alloy layers, suggest that no significant interdiffusion has taken place and also no pronounced melt pool fluctuation occurred during laser manufacturing. Irrespective of the compositional modifications from layer to layer the EBSD cross sectional overview map shown in Figure 2, reveals no substantial associated crystallographic texture differences among the alloys.

This observation shows that the underlying microstructures are similar among layers of different steel composition. This is an advantage associated with the current combinatorial alloy screening method, since direct comparison among different alloys does not get disturbed by differences in crystallographic texture.

The microstructure characteristics and compositions in the different layers can, thus, be efficiently probed from one single cross sectional set of analysis of the multilayered specimen. Time-consuming separate thermo-mechanical treatments, compositional analysis, and metallographic preparation on each individual of the 6 alloy blends can be merged into one single probing step for each technique. This merged approach, thus, enables systematic screening of alloy compositions and their respective properties in a faster way than by conventional synthesizing and processing techniques, where each alloy must be cast and rolled individually.[17,21,22]

Figure 3 shows the microstructure in higher resolution in terms of detailed EBSD maps taken on all individual alloy layers both, before and after the hot rolling procedure.

At this higher EBSD resolution, distinct microstructure differences among the different layers become visible, which can be attributed to the differences in composition and, hence, martensite start temperature.

More specifically, the data reveal that for reference alloy 2, i.e., the CrMoV tool steel and also for the alloy blend consisting of a high fraction of this reference material, i.e., alloy blend 4, the thermomechanical processing leads to a refinement and homogenization of the microstructure. In contrast, for the reference material 1, i.e., the maraging steel and its compositionally nearest blends, particularly for alloy layers 1, 2, and 3, the data show only weak homogenization and a low grain refinement effect. The grain size maps retrieved from the EBSD data show that the grain structure in the near-maraging layers consists of large former austenite crystals, which have been transformed to martensite and, which contain mostly low angle grain boundaries. Similar grain scale subdivision features were observed before also for other maraging steels not produced by LAM.[26,45,46]

EBSD probing also reveals that all alloys exhibit a fully martensitic matrix in the as-synthesized state with the exception of the CrMoV reference tool steel and its nearest alloy blend. These two materials originally contain a small fraction of about 1–5 area% retained austenite, which was removed by the thermomechanical treatment along with the partially dendritic microstructure.

Figure 4 shows the results from microhardness tests, which were performed both in the as-synthesized state, and also after the thermomechanical deformation (50% thickness reduction at 1100 °C) conducted in the dilatometer.

The hardness results show a gradual decrease from the CrMoV reference tool steel toward the maraging reference material and the substrate alloy, which was originally in the soft-annealed state. After deformation and heat treatment, the hardness of the alloy layers is generally slightly lower except for the substrate.

Figure 5a shows the corresponding tensile test results, which match the trends observed from the hardness tests. The observation of the soft and ductile state of the maraging steel is attributed to the fact that the material has not been exposed to the maraging-specific nanoprecipitation treatment, which typically lends it the high hardness for which these alloys are known. The data also reveal that the blends between the two tool steels, i.e., the strong

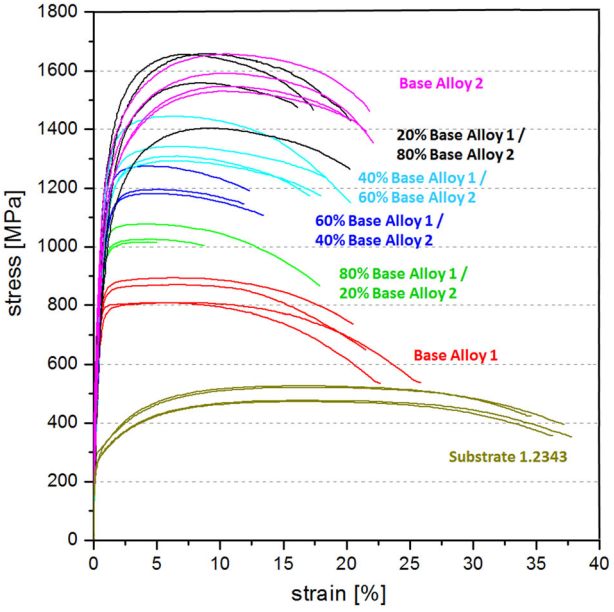

Figure 5. Tensile test results conducted on the deformed and heat treated samples.

CrMoV tool steel on the one hand and the more compliant maraging steel on the other hand, do not entail ductilization of the respective alloys, but lead rather to a reduction in the strain-to-failure.

This effect is attributed to the fact that both tool steels have different optimal precipitation temperatures as well as different martensite grain structure and martensite start temperatures.

4. Conclusions

In this study we showed that LAM can be used efficiently for rapid bulk structural alloy screening. We made the following observations:

1. LMD, which is also referred to as laser cladding is suited to synthesize larger bulk samples with systematically varied composition for conducting combinatorial bulk metallic alloy research. The method allows building up of compositionally piecewise graded materials and in-situ production of new alloys, which are not necessarily made from pre-alloyed metallic powders, rendering it an ideal tool for efficient and rapid alloy development. Further, additional advantages compared to the conventional SLM methods in the context of combinatorial metallurgical synthesis are the high deposition rates and large samples size of the part, which is not limited by a powder-spreading system.
2. The synthesized layered samples reveal excellent chemical and microstructural homogeneity within each compositional layer. Also, all materials, although consisting of different fractions of the respective tool steel powders, revealed comparable crystallographic textures, which renders comparison of the mechanical properties among the different materials straightforward. Similar aspects apply to the retained austenite volume fractions observed in the different layers.
3. An advantage of this approach lies in the fact that the graded bulk specimen, comprising the different alloys, can be jointly deformed in one piece so as to probe corresponding thermomechanical processing pathways.
4. Another advantage, specific of the LMD approach, lies in its capability to synthesize alloy compositions and microstructures that are either not at all or not readily accessible by conventional bulk alloy synthesis. This applies particularly when aiming at conducting combinatorial alloy design for the field of LAM.
5. A shortcoming of the current experiment was that the probed tool steels and their respective alloy blends require different precipitation aging treatments. This means that the global processing applied in the present experiment may potentially not be ideal for some of the probed alloys. This is, however, a limitation, which applies only to a small subset of metallurgical alloys. Also, such alloy blends could be subjected to different heat treatments in order to identify synergies between the corresponding precipitation systems, such as co-precipitation or effects associated with heterogeneous nucleation.
6. Another benefit of the current approach lies in identifying alloys that may potentially reveal better hardness or related beneficial mechanical response in the as-synthesized state compared to their properties after common bulk processing, such as observed, here, for the Dievar alloy.

Received: October 18, 2016; Revised: November 10, 2016

Keywords: laser additive manufacturing; combinatorial synthesis; alloy design; tool steel; maraging steel

References

[1] J. P. Kruth, P. Mercelis, J. van Vaerenbergh, L. Froyen, M. Rombouts, in: *Proc. of the Int. Conf. on Advanced Research in Virtual and Rapid Prototyping* **2003**, p. 59.
[2] M. Rombouts, J. P. Kruth, L. Froyen, P. Mercelis, *CIRP Annals – Manuf. Technol.* **2006**, *55*, 187.
[3] W. E. Frazier, *J. Mater. Eng. Perform.* **2014**, *23*, 1917.
[4] R. J. Herbert, *J. Mater. Sci.* **2016**, *51*, 1165.
[5] S. Nowotny, S. Scharek, E. Beyer, K.-H. Richter, *J. Therm. Spray Technol.* **2007**, *16*, 344.
[6] S. Ocylok, A. Weisheit, I. Kelbassa, *Phys. Procedia* **2010**, *5*, 359.
[7] S. Ocylok, A. Weisheit, I. Kelbassa, *I, Adv. Mat. Res.* **2011**, *278*, 515.
[8] D. Gu, W. Meiners, K. Wissenbach, R. Poprawe, *Int. Mater. Rev.* **2012**, *57*, 133.
[9] P. W. Shindo, F. R. Medina, R. B. Wicker, *J. Mater. Sci. Technol.* **2012**, *28*, 1.
[10] J. P. Kruth, L. Froyen, J. van Vaerenbergh, P. Mercelis, M. Rombouts, B. Lauwers, *J. Mater. Process. Technol.* **2004**, *149*, 616.
[11] D. Gu, Y. C. Hagedorn, W. Meiners, G. Meng, R. J. S. Batista, K. Wissenbach, R. Poprawe, *Acta Mater.* **2012**, *60*, 3849.
[12] F. Abe, K. Osakada, M. Shiomi, K. Uematsu, M. Matsumoto, *J. Mater. Process. Technol.* **2001**, *111*, 210.
[13] D. Herzog, V. Seyda, E. Wycisk, C. Emmelmann, *Acta Mater.* **2016**, *117*, 371.
[14] J.-C. Zhao, *Prog. Mater. Sci.* **2006**, *51*, 557.
[15] J.-C. Zhao, *Adv. Eng. Mater.* **2001**, *3*, 143.
[16] J.-C. Zhao, *J. Mater. Res.* **2001**, *16*, 1565.
[17] H. Springer, D. Raabe, *Acta Mater.* **2012**, *60*, 4950.
[18] D. Raabe, H. Springer, I. Gutierrez-Urrutia, F. Roters, M. Bausch, J. B. Seol, M. Koyama, P. P. Choi, K. Tsuzaki, *JOM* **2014**, *66*, 1845.
[19] K. G. Pradeep, C. C. Tasan, M. J. Yao, Y. Deng, H. Springer, D. Raabe, *Mater. Sci. Eng. A* **2015**, *648*, 183.

[20] Z. Li, K. G. Pradeep, Y. Deng, D. Raabe, C. C. Tasan, *Nature* **2016**, *534*, 227.
[21] H. Springer, M. Beide, D. Raabe, *Mater. Sci. Eng. A* **2013**, *582*, 235.
[22] H. Springer, M. Belde, D. Raabe, *Mater. Des.* **2016**, *90*, 1100.
[23] C. C. Tasan, Y. Deng, K. G. Pradeep, M. J. Yao, H. Springer, D. Raabe, *JOM* **2014**, *66*, 1993.
[24] R. F. Decker, J. T. Eash, A. J. Goldman, *Trans. ASM* **1962**, *55*, 58.
[25] E. V. Pereloma, A. Shekhter, M. K. Miller, S. P. Ringer, *Acta Mater.* **2004**, *52*, 5589.
[26] D. Raabe, D. Ponge, O. Dmitrieva, B. Sander, *Adv. Eng. Mater.* **2009**, *11*, 547.
[27] R. F. Decker, *Source Book on Maraging Steels*, ASM International, Metals Park, OH, **1979**.
[28] D. C. Hofmann, J. Kolodziejska, S. Roberts, R. Otis, R. P. Dillon, J.-O. Suh, Z.-K. Liu, J.-P. Borgonia, *J. Mater. Res.* **2014**, *29*, 1899.
[29] T. Borkar, B. Gwalani, D. Choudhuri, C. V. Mikler, C. J. Yannetta, X. Chen, R. V. Ramanujan, M. J. Styles, M. A. Gibson, R. Banerjee, *Acta Mater.* **2016**, *116*, 63.
[30] B. A. Welk, M. A. Gibson, H. L. Fraser, *JOM* **2016**, *68*, 1021.
[31] A. Reichardt, R. P. Dillon, J. P. Borgonia, A. A. Shapiro, B. W. McEnerney, T. Momose, P. Hosemann, *Mater. Des.* **2016**, *104*, 404.
[32] J. Neidhardt, S. Mraz, J. M. Schneider, E. Strub, W. Bohne, B. Liedke, W. Möller, C. Mitterer, *J. Appl. Phys.* **2008**, *6*, 104.
[33] A. I. Mardare, A. Savan, A. Ludwig, A. D. Wieck, A. W. Hassel, *Electrochem. Acta.* **2009**, *54*, 5973.
[34] T. Lapauw, D. Tytko, K. Vanmeensel, S. Huang, P.-P. Choi, D. Raabe, E. A. N. Caspi, O. Ozeri, M. T. Baben, J. M. Schneider, K. Lambrinou, J. Vleugels, *Inorg. Chem.* **2016**, *55*, 5445.
[35] D. Raabe, F. Roters, J. Neugebauer, I. Gutierrez-Urrutia, T. Hickel, W. Bleck, J. M. Schneider, J. E. Wittig, J. Mayer, *Mrs Bulletin* **2016**, *41*, 320.
[36] A. Abdulkadhim, T. Takahashi, D. Music, F. Munnik, J. M. Schneider, *Acta Mater.* **2011**, *59*, 6168.
[37] J. Cui, Y. S. Chu, O. O. Famodu, Y. Furuya, J. Hattrick-Simpers, R. D. James, A. Ludwig, S. Thienhaus, M. Wuttig, Z. Zhang, I. Takeuchi, *Nat. Mater.* **2006**, *5*, 286.
[38] D. Lencer, M. Salinga, B. Grabowski, T. Hickel, J. Neugebauer, M. Wuttig, *Nat. Mater.* **2008**, *7*, 972.
[39] R. Aparicio-Fernandez, H. Springer, A. Szczepaniak, H. Zhang, D. Raabe, *Acta Mater.* **2016**, *107*, 38.
[40] C. Baron, H. Springer, D. Raabe, *Mater. Des.* **2016**, *97*, 357.
[41] S. Reeh, D. Music, T. Gebhardt, M. Kasprzak, T. Jäepel, S. Zaefferer, D. Raabe, S. Richter, A. Schwedt, J. Mayer, B. Wietbrock, G. Hirt, J. M. Schneider, *Acta Mater.* **2012**, *60*, 6025.
[42] D. Raabe, M. Herbig, S. Sandloebes, Y. Li, D. Tytko, M. Kuzmina, D. Ponge, P. P. Choi, *Curr. Opin. Solid State Mater. Sci.* **2014**, *18*, 253.
[43] M. Kuzmina, M. Herbig, D. Ponge, S. Sandloebes, D. Raabe, *Science* **2015**, *349*, 1080.
[44] M. Kuzmina, D. Ponge, D. Raabe, *Acta Mater.* **2015**, *86*, 182.
[45] D. Raabe, D. Ponge, O. Dmitrieva, B. Sander, *Scr. Mater.* **2009**, *60*, 1141.
[46] O. Dmitrieva, D. Ponge, G. Inden, J. Millan, P. Choi, J. Sietsma, D. Raabe, *Acta Mater.* **2011**, *59*, 364.
[47] H. Zhang, H. Springer, R. Aparicio-Fernandez, D. Raabe, *Acta Mater.* **2016**, *118*, 187.
[48] R. Aparicio-Fernandez, H. Springer, A. Szczepaniak, H. Zhang, D. Raabe, *Acta Mater.* **2016**, *107* 38.
[49] J.-P. Kruth, P. Mercelis, J. van Vaerenbergh, L. Froyen, M. Rombouts, *Rapid Prototyp. J.* **2005**, *11*, 26.
[50] S. S. Al-Bermani, M. L. Blackmore, W. Zhang, I. Todd, *Metall. Mater. Trans. A* **2010**, *41A*, 3422.
[51] L. Thijs, F. Verhaege, T. Craeghs, J. van Humbeeck, J. P. Kruth, *Acta Mater.* **2010**, *58*, 3303.
[52] T. Vilaro, C. Colin, J. D. Bartout, *Metall. Mater. Trans. A* **2011**, *42*, 3190.
[53] H. Attar, M. Calin, L. C. Zhang, S. Scudino, J. Eckert, *Mater. Sci. Eng. A* **2014**, *593*, 170.
[54] X. Tan, Y. Kok, Y. J. Tan, M. Descoins, D. Mangelinck, S. B. Tor, K. F. Leong, C. K. Chua, *Acta Mater.* **2015**, *97*, 1.
[55] D. A. Ramirez, L. E. Murr, E. Martinez, D. H. Hernandez, J. L. Martinez, B. I. Machado, F. Medina, P. Frigola, R. B. Wicker, *Acta Mater.* **2011**, *59*, 4088.
[56] H. D. Carlton, A. Haboub, G. F. Gallegos, D. Y. Parkinson, *Mater. Sci. Eng. A* **2016**, *651*, 406e414.
[57] S. Dadbaksh, L. Hao, N. Sewell, *Rapid Prototyp. J.* **2012**, *18*, 241e249.
[58] K. Kempen, E. Yasa, L. Thijs, J. P. Kruth, J. van Humbeeck, *Phys. Proc.* **2011**, *12*, 255e263.
[59] E. A. Jägle, P. P. Choi, J. van Humbeeck, D. Raabe, *J. Mater. Res.* **2014**, *29*, 2072.
[60] J. Kranz, D. Herzog, C. Emmelmann, *J. Laser Appl.* **2015**, *27*, S14001.
[61] B. van der Schueren, J. P. Kruth, *Rapid Prototyp. J.* **1995**, *1*, 23e31.
[62] K. Schmidtke, F. Palm, A. Hawkins, C. Emmelmann, *Phys. Procedia* **2011**, *12*, 369.
[63] K. Mahmood, A. J. Pinkerton, *J. Eng. Manuf.* **2013**, *227*, 520e531.
[64] S. Ocylok, A. Weisheit, I. Kelbassa, *Adv. Mat. Res.* **2011**, *278*, 515.
[65] J. Mazumder, J. Choi, K. Nagarathnam, J. Koch, D. Hetzner, *JOM* **1997**, *49*, 55.
[66] M. Cabeza, G. Castro, P. Merino, G. Pena, M. Román, *Surf. Coat. Technol.* **2012**, *212*, 159.
[67] K. Kempen, E. Yasa, L. Thijs, J.-P. Kruth, J. van Humbeeck, *Phys. Procedia* **2011**, *12*, 255.

[68] G. Casalino, S. L. Campanelli, N. Contuzzi, A. D. Ludovico, *Opt. Laser Technol.* **2015**, *65*, 151.
[69] D. Raabe, M. Sachtleber, H. Weiland, G. Scheele, Z. S. Zhao, *Acta Mater.* **2003**, *51*, 1539.
[70] Z. Zhao, M. Ramesh, D. Raabe, A. M. Cuitino, R. Radovitzky, *Int. J. Plast.* **2008**, *24*, 2278.
[71] M. Sachtleber, Z. Zhao, D. Raabe, *Mater. Sci. Eng. A* **2002**, *336*, 81.
[72] D. Raabe, M. Sachtleber, Z. Zhao, F. Roters, S. Zaefferer, *Acta Mater.* **2001**, *49*, 3433.
[73] C. Sachs, H. Fabritius, D. Raabe, *J. Struct. Biol.* **2006**, *155*, 409.
[74] A. Godara, D. Raabe, *Nondestr. Test. Eval.* **2008**, *23*, 229.
[75] A. Godara, D. Raabe, I. Bergmann, R. Putz, U. Mueller, *Compos. Sci. Technol.* **2009**, *69*, 139.